JURNAL TEKNIK SIPIL
Jurnal Teoretis dan Terapan Bidang Rekayasa Sipil

Vorticity Fields on Flow with Vortex System

Bambang Yulistiyanto

Civil and Environmental Engineering Department, Faculty of Engineering, Gadjah Mada University
Jl. Grafika 2 Yogyakarta 55281, E-mail: yulis@tsipil.ugm.ac.id

Abstract

The flow around a circular cylinder mounted normal to the channel bed is essentially a three-dimensional one. The flow upstream undergoes a separation of the turbulent boundary layer and rolls up to form a flow system, known as horseshoe vortex, which is swept around the cylinder. This vortex system plays an important role, if the bed material is movable. The shear stress of the vortex system is responsible to the bed erosion. The shear stress depends on the velocity gradient, may be presented as the vorticity. This study is done to gain a better understanding of the vorticity around a cylinder, especially where the system of vortices exist. Flow measurements were used to study the vorticity fields on flow with a horse-shoe vortex system around a pile. The velocity vector plots show the presence of a primary vortex upstream of the cylinder. Based on these velocity vectors, the vorticity can be analyzed by using central finite difference approximations. Results of the vorticity calculation are presented as the vorticity contours. Results of study show the greatest value of the positive-vorticity on the horse-shoe vortex system is in the plane upstream of cylinder. This value decreases in the planes downstream, attaining the lowest value in the plane downstream, where the wake vortex established. The strength of the positive vorticity increases at larger Reynolds number. Underneath the field of positive vorticity, stretching around the cylinder, it appears a field of negative vorticity. This negative vorticity near the bed is high in front of the cylinder, proportional to the bed shear stress, which is responsible to the development of local scour at the movable bed. The line of zero vorticity is plotted originated at the bed, being as the separation point. It is also concluded that the maximum positive-vorticity is not necessary coincided with the center of the vortex.

Keywords: *Horse-shoe vortex system, vorticity, Reynolds number.*

Abstrak

Pola aliran di sekitar silinder bulat yang dipasang tegak lurus dasar saluran merupakan aliran tiga dimensi Aliran di hulu silinder membentuk separasi pada lapis batas turbulen, membangkitkan terbentuknya pusaran tapal-kuda yang mengelilingi silinder. Sistem pusaran ini mempunyai peranan penting jika material dasar mudah bergerak. Tegangan geser pada sistem pusaran akan menyebabkan terbentuknya erosi lokal. Besarnya tegangan geser bergantung pada perbedaan kecepatan, yang dapat dipresentasikan dengan nilai vortisitasnya. Studi ini bertujuan untuk mendapatkan pemahaman yang lebih baik tentang vortisitas di sekitar silinder, terutama di lokasi dimana terbentuk system vortex. Data hasil pengukuran kecepatan aliran dipakai untuk mempelajari system vortisitas pada aliran dengan sistem pusaran di sekitar pilar. Gambar vektor kecepatan di sekitar pilar silinder memperlihatkan keberadaan pusaran utama di depan silinder. Berdasarkan vector kecepatan tersebut, dapat dianalisis vortisitasnya dengan menggunakan metode beda hingga. Hasil hitungan vortisitas digambarkan dalam bentuk kontur vortisitas. Hasil studi menunjukkan nilai maksimum dari vortisitas positif (searah jarum jam) dari sistem pusaran tapal kuda adalah pada bidang simetri di hulu silinder. Nilai vortisitas tersebut menurun, mencapai nilai minimum di hilir silinder. Besarnya vortisitas positif meningkat pada angka Reynold yang lebih tinggi. Di bawah bidang vortisitas positif, diperlihatkan terbentuknya system vortisitas negatif. Vortisitas negative di dekat dasar di depan silinder mempunyai nilai yang besar, proporsional dengan nilai tegangan geser di dasar, yang bertanggungjawab pada terbentuknya erosi lokal pada saluran dengan dasar bergerak. Garis yang memberikan nilai vortisitas sama dengan nol, merupakan garis separasi antara vortisitas positif dan negative. Dari hasil kajian juga disimpulkan bahwa posisi dari vortisitas positif maksimum tidak selalu berimpit dengan pusat pusaran tapal kuda.

Kata-kata Kunci: *Sistem pusaran tapal kuda, vortisitas, angka Reynolds.*

1. Introduction

The flow field in a shear flow around a circular cylinder mounted normal to the channel bed is essentially a three-dimensional one. This type of flow is the result of the interaction between the two-dimensional undisturbed shear flow and the cylinder in the region of the pressure gradient set up by the cylinder. The flow upstream undergoes a separation of the turbulent boundary layer and rolls up to form a flow system, known as horseshoe vortex, which is swept around the cylinder. This vortex system plays an important role, if the bed material is movable. The shear stress of the vortex system may be responsible to the bed erosion. The shear stress depends on the velocity gradient, may be presented as the vorticity.

Yulistiyanto, 1997, studied numerically flow fields around a cylinder and verified by experimental study to find velocity distribution in longitudinal, transversal and vertical directions. It was also presented the turbulence intensities, which is moderate in front of the cylinder, but increases enormously behind the cylinder, due to the fluctuations in the wake vortex. The flow upstream undergoes a separation of the turbulent boundary layer and rolls up to form a flow system, known as horseshoe vortex, which is swept around the cylinder (Yulistiyanto, 2009). The flow around a vertical circular pile exposed to a steady current is studied experimentally. Yulistiyanto, 2009, showed the present of the vertical velocities distributions of the flow around a cylinder, showing a highly three-dimensional picture, being reasonably organized in the front and less organized in the back of the cylinder, where flow separation takes place. It also shows that a horseshoe-vortex system is established, existing of a measurable vortex with underneath a return flow. This type of flow occurs in a variety of situations, such as flow around bridge piers, around buildings and structures, and at different types of junctions. The horseshoe-vortex system plays an important role, if the bed material is movable. The shear stress of the vortex system may be responsible to the bed erosion. In this paper, this shear stress will be presented as the vorticity, containing the gradient of the velocity distributions.

Studies of vorticity fields were performed using numerical and visual methods (Green and Gerrard, 1993; Okude and Matsui 1989). The author investigates vorticity around a cylinder based on three dimensional velocity measurements in radial directions to the cylinder. This gives a better understanding about the complexity of flow fields around a cylinder.

2. Velocity Measurements

Experiment measurements were conducted by Abdul Barbhuiya and Dey (2003), for flow around a vertical semicircular cylinder attached to the sidewall and at a wing-wall abutment installed at a rectangular channel, and by Andreas Roulund at.al. (2005). Flow fields upstream of an obstacle was explored by Graf and Yulistiyanto (1997), showed development of vortex upstream from the cylinder. Velocities around a cylinder were investigated experimentally (Dargahi, 1989; Yulistiyanto, 1997 and 2009), results the velocity distributions in different planes upstream and downstream from a cylinder. Two tests have been performed by Yulistiyanto, 1997, and whose hydraulic characteristics are given in **Table 1**.

The experiments were performed in a 43.0 [m] long and 2.0 [m] wide tilting flume. An Acoustic Doppler Velocity Profiler (ADVP) was used to measure the velocities. Detailed information on the experimental installation and experimental results are found elsewhere (Yulistiyanto, 1997 and 2009).

3. Velocity Distributions

Instantaneous velocities distributions, $u(z)$, $v(z)$, $w(z)$, were measured at different points, $P(x,y,z)$ or $P(r,\alpha,z)$, in the range of $12<r[cm]<44$ and $0<\alpha[°]<180$ around the cylinder; the origin was positioned in the centre of the cylinder, $P(0,0,z)$, whose radius is $r=11[cm]$. The vertical distributions of the velocities for Test 1 are presented in **Figure 1**. For Test 2, they are showed in axonometric form in **Figure 2** (Yulistiyanto, 2009).

Table 1. Flow variables and channel parameters

	Cylinder		Channel:uniform flow B = 2.0 [m]								
Test	D [m]	Re_D 10^5	Q [m³/dt]	S_o 10^{-4}	n [m$^{-1/3}$s]	U_∞ [m/dt]	h_∞ [m]	B/h	U_{*cr} [m/dt]	Re_h 10^5	Fr
1	0.22	1.48	0.248	6.25	0.012	0.67	0.185	10.8	0.029	1.24	0.5
2	0.22	0.95	0.149	2.80	0.012	0.43	0.173	11.6	0.021	0.74	0.33

(Source: Yulistiyanto, 1997)
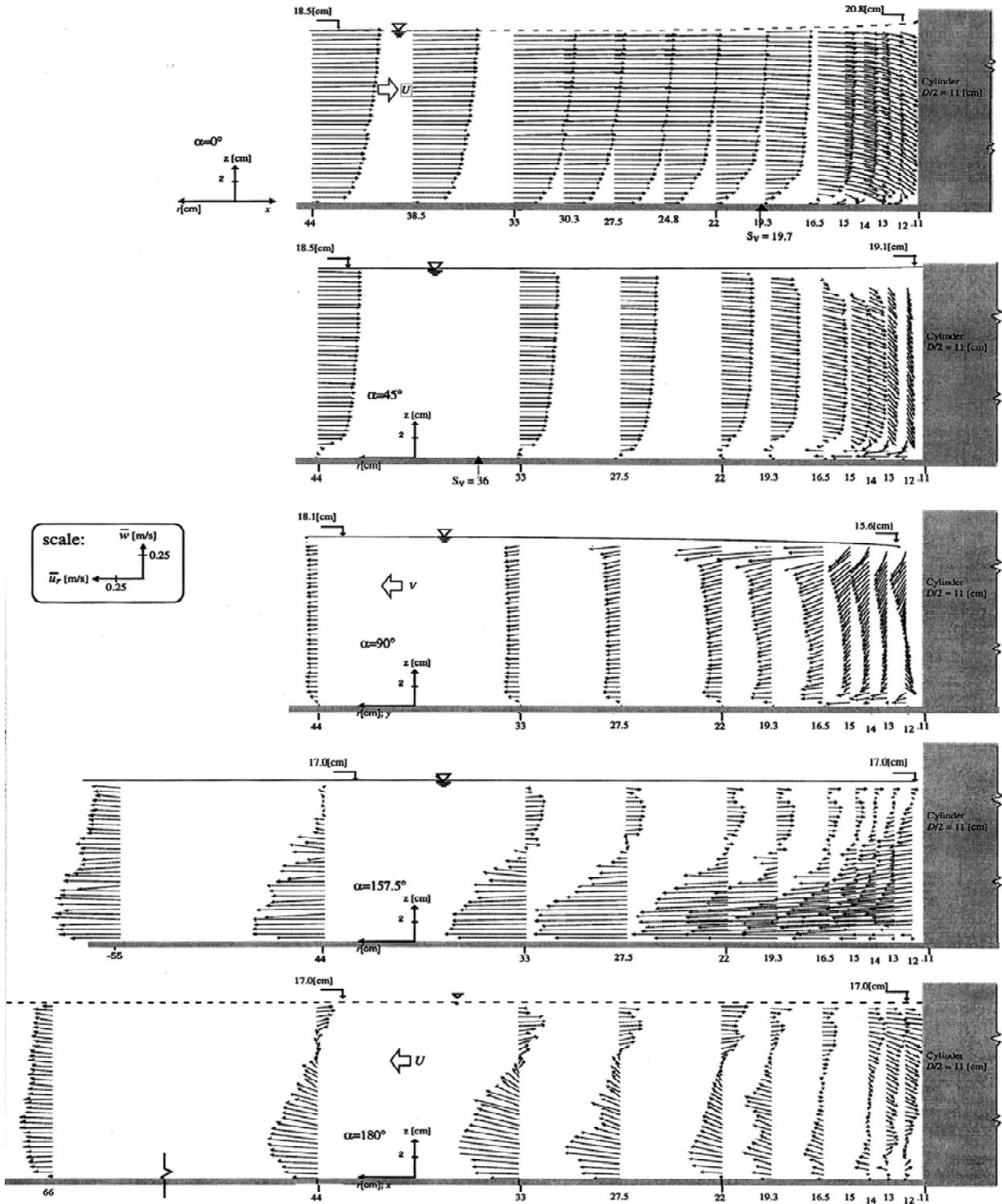
Figure 1. Velocity Vectors, $\overline{u}_r$, $\overline{w}$, in Planes 0°, 45°, 90°, 157.5°, and 180°, for Test 1
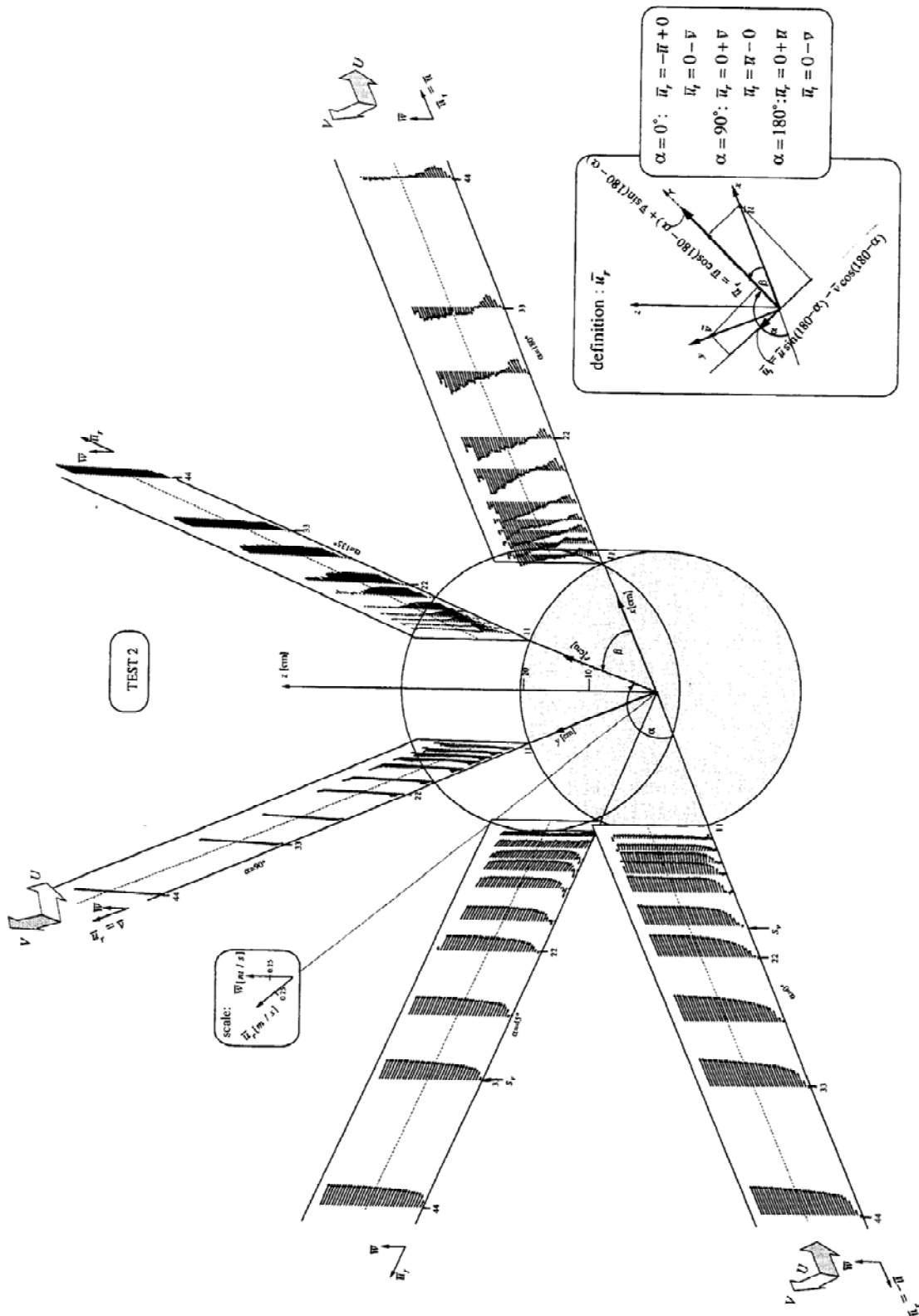
Figure 2. Axonometric representation of flow in planes around a cylinder, for test 2

4. Discussion

4.1 Streamwise vorticity

From the velocity distributions, it is evident that a vorticity, ω_t, exists, to be calculated as :

$$\omega_t = \frac{\partial \overline{u}_r}{\partial z} - \frac{\partial \overline{w}}{\partial r} \tag{1}$$

Using **Equation 1**, it is possible now to compute the vorticity components, ω_t (central finite difference approximations are used). This is illustrated in **Figure 3** and **Figure 4** for both tests, each is for the five planes. Note, that only a sub domain near the bed, 12 < r [cm] < 44 and 0 < z [cm] < 4, has here been evaluated.

In **Figure 3** and **Figure 4**, it can be seen that a system of vorticity of different strength is noticeable. However a positive vorticity shows a pronounced design. The location, $C+$, of the maximum positive vorticity, $\omega_t^{max(+)}$, is given for :

Plane 0° :
  Test 1: $\omega_t^{max(+)} = 70$ [s^{-1}] at $C+$ ($r/D = 0.67$; $z/D = 0.029$)
  Test 2: $\omega_t^{max(+)} = 21$ [s^{-1}] at $C+$ ($r/D = 0.74$; $z/D = 0.060$)

Plane 45° :
  Test 1: $\omega_t^{max(+)} = 34$ [s^{-1}] at $C+$ ($r/D = 0.57$; $z/D = 0.080$)
  Test 2: $\omega_t^{max(+)} = 25$ [s^{-1}] at $C+$ ($r/D = 0.66$; $z/D = 0.039$)

Plane 90° :
  Test 1: $\omega_t^{max(+)} = 25$ [s^{-1}] at $C+$ ($r/D = 0.58$; $z/D = 0.070$)
  Test 2: $\omega_t^{max(+)} = 10$ [s^{-1}] at $C+$ ($r/D = 0.82$; $z/D = 0.060$)

Plane 157.5° (135°) :
  Test 1: $\omega_t^{max(+)} = 20$ [s^{-1}] at $C+$ ($r/D = 0.60$; $z/D = 0.159$)
  Test 2: $\omega_t^{max(+)} = 10$ [s^{-1}] at $C+$ ($r/D = 0.58$; $z/D = 0.182$)

Plane 180° :
  Test 1: $\omega_t^{max(+)} = 14$ [s^{-1}] at $C+$ ($r/D = 0.63$; $z/D = 0.048$)
  Test 2: $\omega_t^{max(+)} = 8$ [s^{-1}] at $C+$ ($r/D = 1.35$; $z/D = 0.126$)

The greatest value of the $\omega_t^{max(+)}$ is in the plane 0° for Test 1, for Test 2, the $\omega_t^{max(+)}$ in the plane 0° and 45° is not much different, being equal to 21 – 25 [s^{-1}]. This value decreases in the planes downstream, attaining the lowest value in the plane 180°. The $\omega_t^{max(+)}$ for Test 1 are bigger than the ones for Test 2. This concludes that the strength of the positive vorticity increases at larger Reynolds number.

Underneath the field of positive vorticity, stretching around the cylinder, is what it appears to be a field of negative vorticity. The location, $C-$, of the maximum negative vorticity, $\omega_t^{max(-)}$, is given for :

Plane 0° :
  Test 1: $\omega_t^{max(-)} = -24$ [s^{-1}] at C- ($r/D = 0.81$; $z/D = 0.0$)
  Test 2: $\omega_t^{max(-)} = -20$ [s^{-1}] at $C-$ ($r/D = 0.65$; $z/D = 0.0$)

Plane 45° :
  Test 1: $\omega_t^{max(-)} = -30$ [s^{-1}] at $C-$ ($r/D = 0.79$; $z/D = 0.0$)
  Test 2: $\omega_t^{max(-)} = -32$ [s^{-1}] at $C-$ ($r/D = 0.65$; $z/D = 0.0$)

Plane 90° :
  Test 1: $\omega_t^{max(-)} = -40$ [s^{-1}] at $C-$ ($r/D = 0.68$; $z/D = 0.0$)
  Test 2: $\omega_t^{max(-)} = -30$ [s^{-1}] at $C-$ ($r/D = 0.69$; $z/D = 0.0$)

Plane 157.5° (135°):
  Test 1: $\omega_t^{max(-)} = -20$ [s^{-1}] at $C-$ ($r/D = 0.95$; $z/D = 0.044$)
  Test 2: $\omega_t^{max(-)} = -40$ [s^{-1}] at $C-$ ($r/D = 1.05$; $z/D = 0.039$)

Plane 180° :
  Test 1: $\omega_t^{max(-)} = -50$ [s^{-1}] at $C-$ ($r/D = 1.37$; $z/D = 0.0$)
  Test 2: $\omega_t^{max(-)} = -14$ [s^{-1}] at $C-$ ($r/D =1.33$; $z/D = 0.039$)

The values of $\omega_t^{max(-)}$ for Test 1 are bigger than the ones for Test 2, except in the plane 45° and in the plane 157.5° which has a smaller value than in plane 135°. The regions of the negative vorticity increase in size in planes downstream, however their strengths are not necessary increased. The existence of the reversal flow very close to the bed, in front of the cylinder (planes 0° and 45°), should give the negative shear stress, presented as the negative vorticity. It was reported that the beginning of the scour is not at the upstream of the cylinder, showed by the highest value of the negative vorticity, located near the bed, in plane 45° for Test 2 and in plane 90° for Test 1. In plane 135° for Test 2, the $\omega_t^{max(-)}$ is high, however its location is far from the bed, at $z/D = 0.039$. For Test 1, in plane downstream, its value is also high, however its locations is far enough from the cylinder, $r/D = 1.37$.

The presence of the horseshoe vortex in front of the cylinder can be seen, containing a single vortex which is a clockwise rotating as shown in the region of the positive vorticity. This vortex passing out of the vertical plane and proceeding tangentially around the cylinder, washing away in downstream direction. Underneath this vortex, there is a reverse flow, produced the negative vorticity. If the bed of the channel is mobile, it is probable that the strong of the negative vorticity does the erosion, while the vortex with positive vorticity participates in the transportation of sediments.

$$Streamwise\ vorticity: \frac{\partial \overline{u}_r}{\partial z} - \frac{\partial \overline{w}}{\partial r} = \omega$$
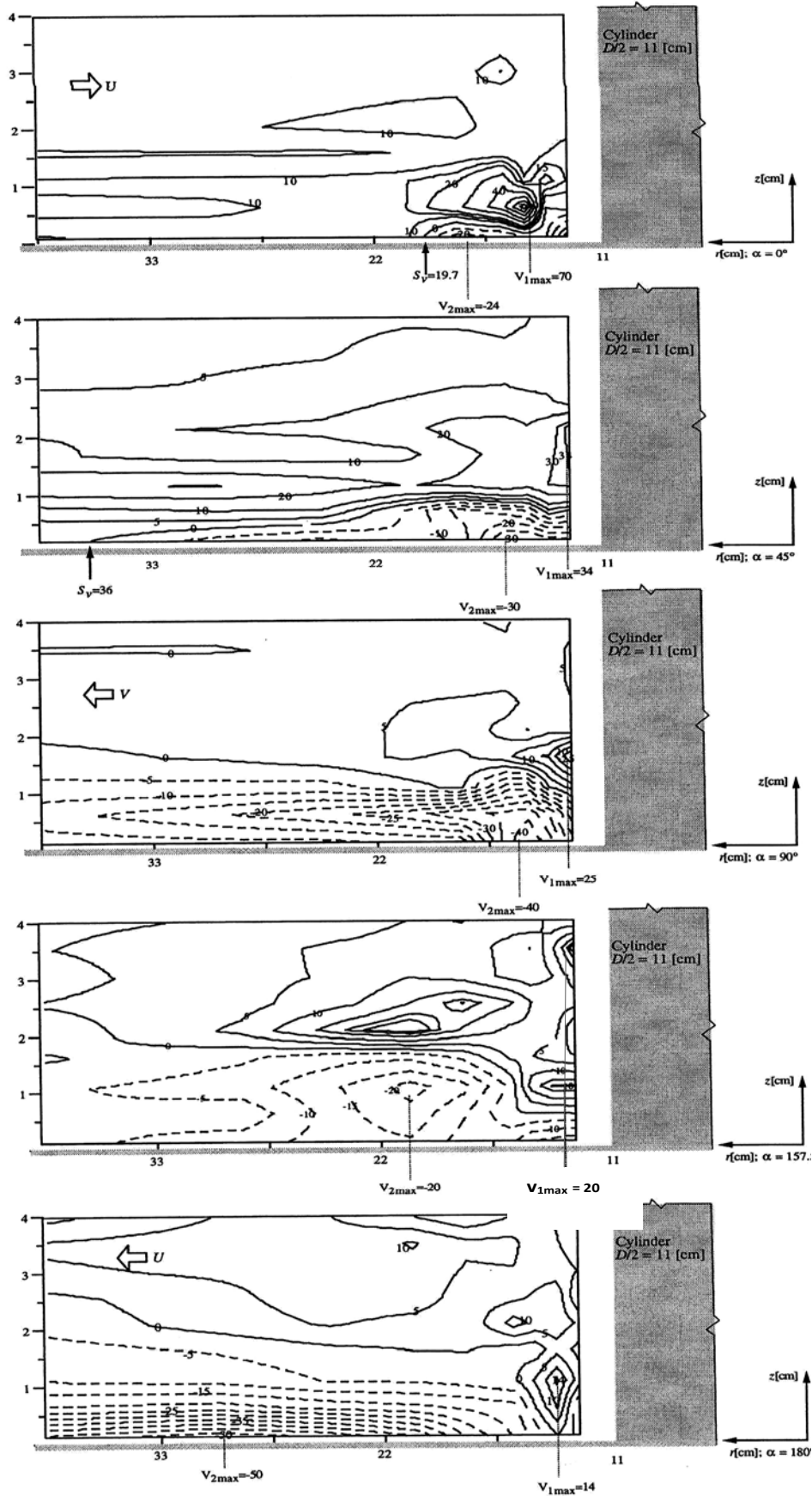

Figure 3. Vorticity contours in 5 different planes for test 1

$$\textit{Streamwise vorticity}: \frac{\partial \bar{u}_r}{\partial z} - \frac{\partial \bar{w}}{\partial r} = \omega$$
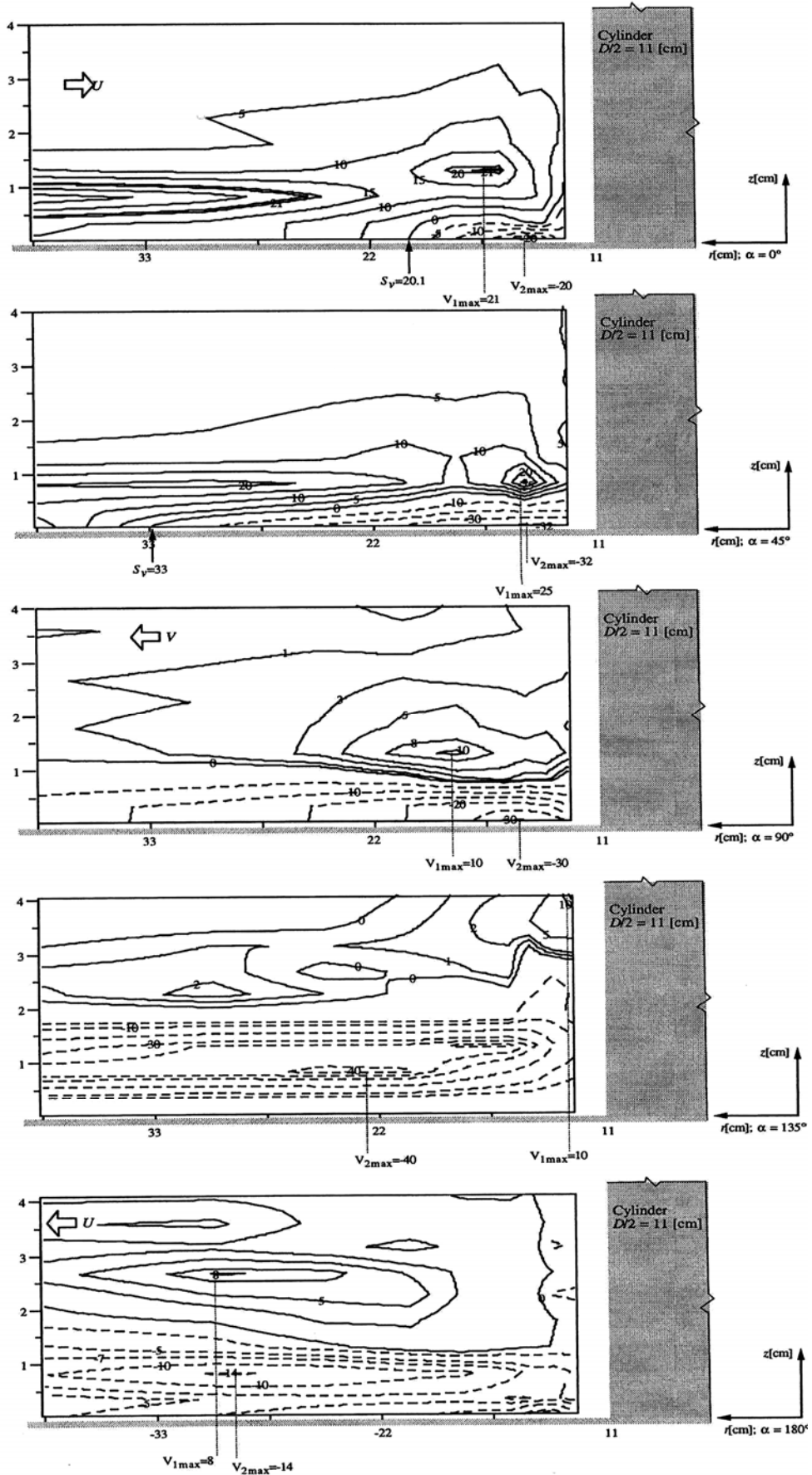

Figure 4. Vorticity contours in 5 different planes for test 2

4.2 Connection between the radial velocity the vorticity field

Figure 5 shows the connection between the radial velocity, $\bar{u}_r$, and the vorticity field, ω. For the sake of simplificity a parallel flow is considered in **Figure 5**. Due to the pressure gradient, $dp/dx > 0$, there exists a point for which the vertical velocity gradient is zero at the bed, $(\partial \bar{u}/\partial z)_{z=0} = 0$, at which the water close to the bed is not able to travel along the bed and separates from it. This position is called the separation point, which is defined as a point of transition from the forward and reverse flow. The flow upstream of the separation point is not much affected by separation, but the flow downstream of the separation point changes, showing reverse flow.

From the measured velocity distributions, $\bar{u}(z)$, the vorticity distribution, $\partial \bar{u}/\partial z(z)$, can becomputed, subsequently the vorticity contours are obtained. It can be seen, that a clockwise vortex, *V*, containing positive vorticity, and a reverse flow in the underneath, containing negative vorticity, are created.

The line of $\omega_t = 0$ coincides with the maximum reverse velocity. The regions above and under this line have always positive and negative vorticity, respectively.

Above this line, there is a line of $\bar{u}(z) = 0$, indicating the centre of the vortex.

The maximum positive vorticity is defined as $\partial^2 \bar{u}/\partial z^2 = 0$ being as the point of inflexion (PI). The position of this inflexion point is not necessary coincided with the point of $\bar{u}(z) = 0$.

Relations between the radial velocity and the vorticity described in **Figure 5** can readily be observed in the measured velocity and calculated vorticity fields, shown in **Figures 6, 7**, and and **8** for the both tests in the planes $\alpha = 0°$, $\alpha = 45°$ and $\alpha = 90°$. Here the flow is no more parallel, the streamlines are curved. The velocity distributions show clearly the flow reversal, while the vorticity distributions show to be the expected shape, given with **Figure 5**.

The line of $\bar{u}_r = 0$ and the line of $w_t = 0$ are also plotted together with the separation line in **Figure 6** to **8**. These lines are originated at the bed, being as the separation point, *Sv*. At region near the leading edge of the cylinder, the gradient of the vertical velocity is always less then zero, $d\overline{w}/dx < 0$, consequently, according to **equation. 1**, the position of $w_t = 0$ is under the maximum reverse velocity. This line slightly climbs up in planes downstream. The lines of $\bar{u}_r = 0$ in planes 0° and 45° are under the maximum positive vorticity (being as the position of the point inflexion). The separation line between the vortex region and the main flow is traced approximatively.

The separation points in planes $\alpha = 0°$ and $\alpha = 45°$ for the both tests are situated at (see **Figures 6** and **7**):
Plane 0° :

   Test 1: *Sv* (r/D = 0.90 ; z/D = 0.0)

   Test 2: *Sv* (r/D = 0.91 ; z/D = 0.0)

Plane 45° :

   Test 1: *Sv* (r/D = 1.65 ; z/D = 0.0)

   Test 2: *Sv* (r/D = 1.50 ; z/D = 0.0)

At the other planes, the position of the separation points could not be defined, presumed far enough from the cylinder, $r/D > 2$. These data show that the region of the negative vorticity increases in size and the position of the separation point is farther in plane downstream.
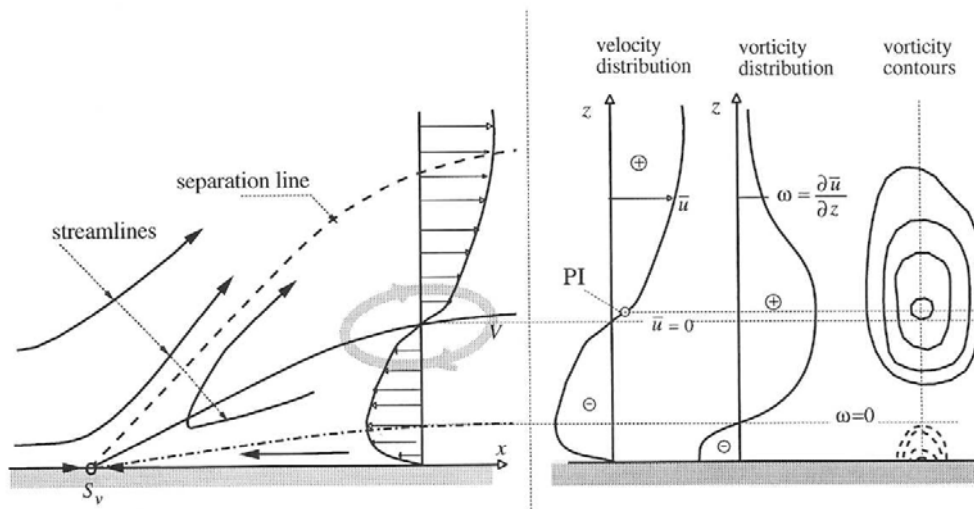

Figure 5. Connection between the radial velocity, $\bar{u}_r$, and the vorticity field, ω

$$\text{scale}: \quad \underline{\hspace{1.5cm}} \quad \omega = \frac{\partial \bar{u}_r}{\partial z} - \frac{\partial \bar{w}}{\partial r} = 30 [s^{-1}] \quad ; \quad \longrightarrow \quad \begin{array}{l} \bar{u}_r = 0.5 \ [m/s] \\ \bar{w} = 0.5 \ [m/s] \end{array}$$

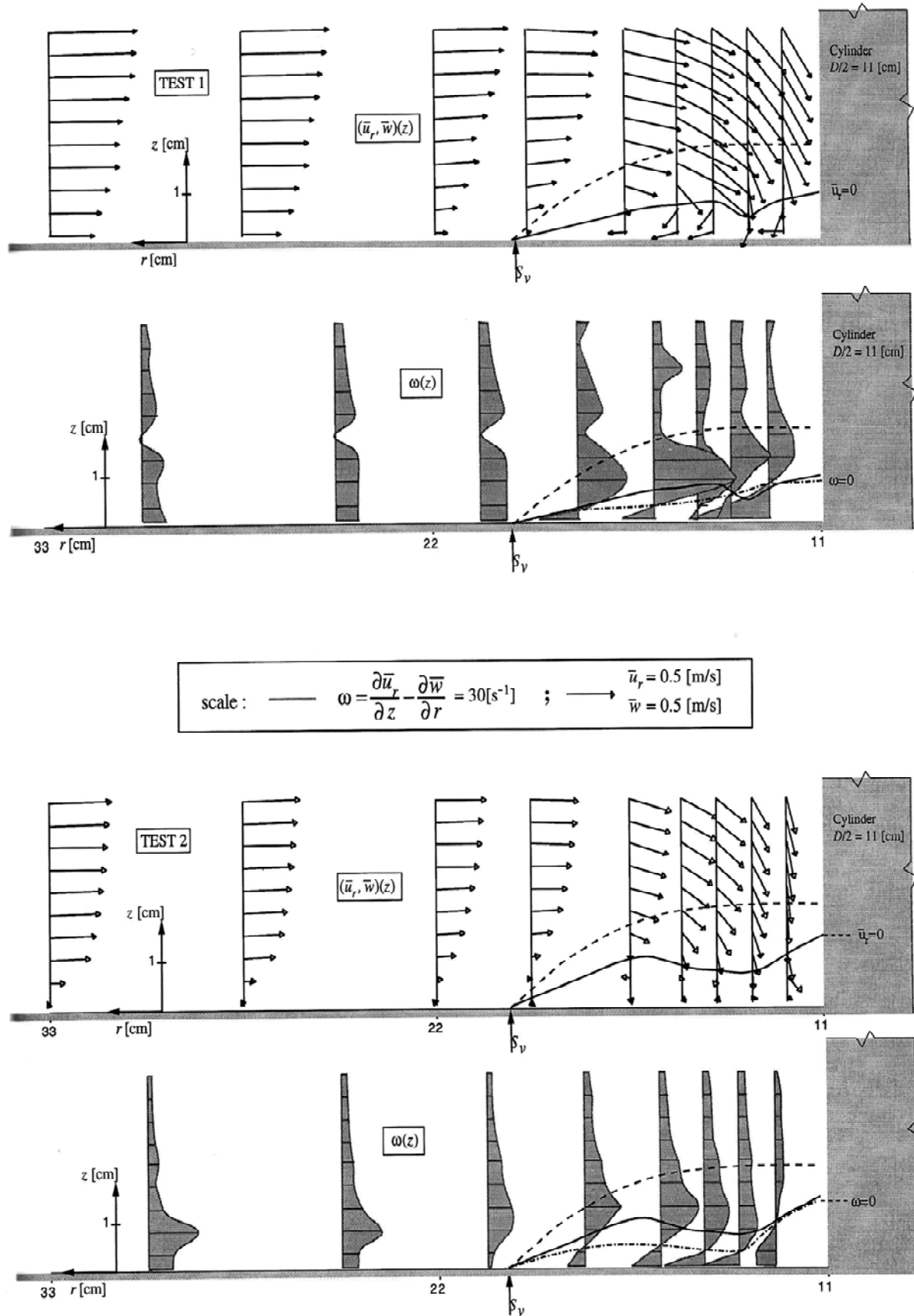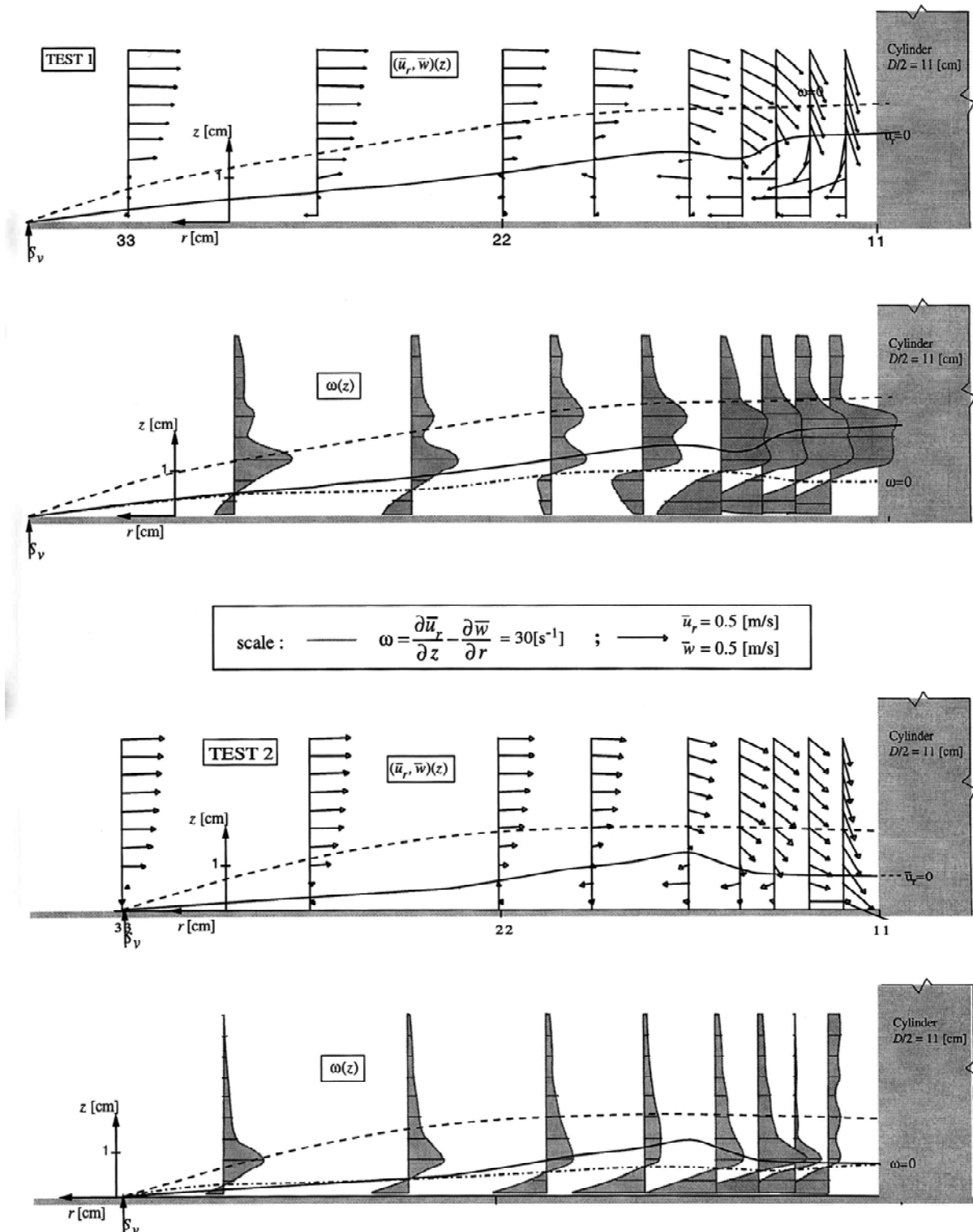**Figure 6. Radial velocity and vorticity fields in plane upstream, $\alpha = 0^o$, for both tests**

Figure 7. Radial velocity and vorticity fields in plane $\alpha = 45^{\circ}$, for both tests

$$\text{scale}: \quad \underline{\qquad} \quad \omega = \frac{\partial \overline{u}_r}{\partial z} - \frac{\partial \overline{w}}{\partial r} = 30[\text{s}^{-1}] \quad ; \quad \longrightarrow \quad \begin{array}{l} \overline{u}_r = 0.5 \ [\text{m/s}] \\ \overline{w} = 0.5 \ [\text{m/s}] \end{array}$$
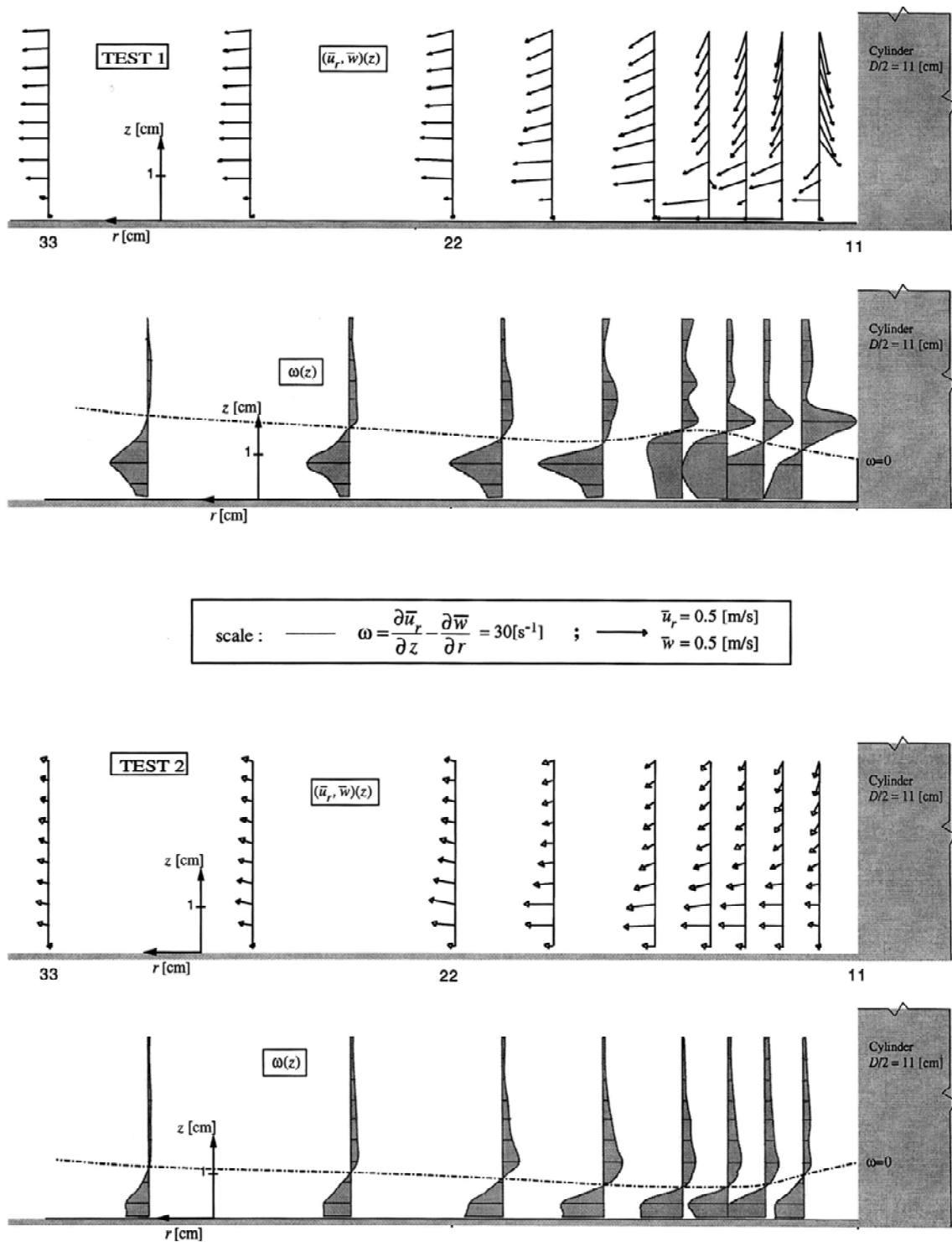
Figure 8. Radial Velocity and Vorticity Fields in Plane $\alpha = 90^{\circ}$, for Both Tests

5. Conclusions

Measurements of flow structure upstream and around a cylinder were reported for fully developed turbulent open-channel flow at $Re_D=10^5$, resulting the three-dimensional velocity profiles. From these velocity distributions, the vorticity distribution can be computed, subsequently the vorticity contours are obtained. It can be seen, that a clockwise vortex, containing positive vorticity, and a reverse flow in the underneath, containing negative vorticity, are created. The vorticities are presented as vorticity contours at five different planes around a cylinder. It can be seen that a system of vorticity of different strength is noticeable, which a positive vorticity shows a pronounced design. Its greatest value is in the upstream plane, and their value decrease in the planes downstream, attaining the lowest value in the plane 180°. It is also showed the existence of a reverse flow, produced the negative vorticity. If the bed of the channel is mobile, it is probable that the strong of the negative vorticity does the erosion, while the vortex with positive vorticity participates in the transportation of sediments. The line of zero vorticity is also plotted originated at the bed, being as the separation point, *Sv*.

Notations

a	= Distance of the separation point from the edge of the cylinder;
D	= Diameter of cylinder;
$C+$, $C-$	= Position of maximum vorticity;
h_∞	= Depth of uniform flow;
Q	= Discharge;
r	= Distance of point from center of cylinder;
Re_h	= Flow Reynolds number;
S_v	= Separation point;
u_{*x}	= Longitudinal friction velocity;
U_∞	= Longitudinal uniform velocity;
$\overline{u}$, $\overline{v}$, $\overline{w}$	= Longitudinal, transversal, and vertical point velocities;
$\overline{u}_r$	= Radial velocity;
x, y, z	= Longitudinal, transversal, and vertical coordinates;
α	= Radial direction of plane;
ω_t	= Tangential vorticity;

References

Barbhuiya, A.B. and Dey, S., 2003, Measurement of Turbulent Flow Field at a Vertical Semicircular Cylinder Attached to the Sidewall of a Rectangular Channel, *Flow Measurement and Instrumentation*, Volume 15, Issue 2, April 2004, Pages 87-96, Elsevier.

Andreas, R, Sumer, B.M., Jorgen, F., and Jess, M., 2005, Numerical and Experimental Investigation of Flow and Scour Around a Circular Pile, *Journal of Fluid Mechanics*, 534:351-401, Cambridge.

Dargahi, B., 1989, The Turbulent Flow Fields Around a Circular Cylinder, *Experiments in Fluids*, Vol. 8, pp. 1-12.

Graf, W.H. and Yulistiyanto, B., 1997, Experiments on Flow Upstream of a Cylinder, San Francisco, USA: *PROC., XXVII Congr., Int. Assoc. Hydr. Res.,* Vol. 1.

Green, R.B., and Gerrard, J.H., 1993, Vorticity Measurements in the Near Wake of a Circular Cylinder at Low Reynolds Numbers, *Journal of Fluid Mechanics.*

Okude, M., and Matsui, T., 1989, Vorticity Distribution of Vortex Street in the Wake of a Circular Cylinder, Japan Society for Aeronautical and Space Sciences. Japan: *Journal* (ISSN 0021-4663), Vol. 37, No. 431.

Yulistiyanto, B., 1997, *Flow Around a Cylinder Installed in a Fixed-bed Open Channel*, Ph.D Dissertation 1631, Ecole Polytechnique Federale, Lausanne, CH.

Yulistiyanto, B., 2009, Velocity Measurements on Flow Around a Cylinder, Indonesia: *Dinamika Teknik Sipil*, Vol. 10.